Inorganic Chemistry

Article

pubs.acs.org/IC

Synthesis and Electrochemical and Photophysical Properties of Calixarene-Based Ruthenium(II) Complexes as Potential Multivalent Photoreagents

Alice Mattiuzzi,[†] Lionel Marcélis,[‡] Ivan Jabin,*[,†] Cécile Moucheron,*[,‡] and Andrée Kirsch-De Mesmaeker*[,‡]

[†]Laboratoire de Chimie Organique, Université libre de Bruxelles, Avenue F. D. Roosevelt 50, CP160/06, B-1050 Brussels, Belgium

[‡]Laboratoire de Chimie Organique et Photochimie, Université libre de Bruxelles, Avenue F. D. Roosevelt 50, CP160/08, B-1050 Brussels, Belgium

Supporting Information

ABSTRACT: The grafting of photoreactive and photooxidizing $Ru^{II}(TAP)$ (TAP = 1,4,5,8-tetraazaphenanthrene) complexes on calix[4 or 6]arene molecular platforms is reported. Thus, either $[Ru(TAP)_2(phen)]^{2+}$ (phen = 1,10-phenanthroline) or $[Ru(TAP)_2(pytz)]^{2+}$ [pytz = 2-(1,2,3-triazol-4-yl)pyridine] complexes are anchored to the calixarenes. The data in electrochemistry, combined with those in emission under steady state and pulsed illumination and the determination of the associated photophysical rate constants, indicate the presence of intramolecular luminescence quenching by the phenol moieties of calixarene. From transient absorption studies under pulsed laser irradiation, it is concluded that the quenching originates from a par proton-coupled electron transfer (PCET) process. Such an intramolecular quenching is absent when the phenol groups of the calixarene platform are derivatized by azido arms.

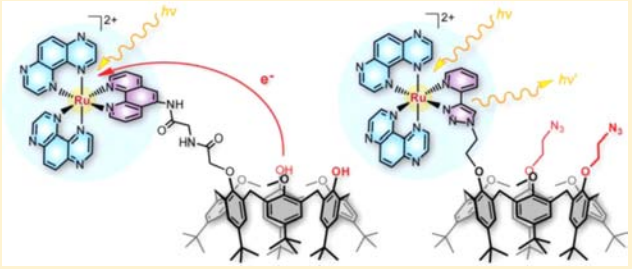

INTRODUCTION

The photophysical and photochemical properties of ruthenium(II) polypyridyl complexes continue to attract much attention particularly for the development of various applications such as the design of antenna systems for collecting light.[1−5] In addition, some ruthenium(II) polyazaaromatic complexes are characterized by a long-lived visible luminescence very sensitive to the microenvironment. Therefore, they can also be used as photoprobes, in particular of genetic material and may be considered as potential drugs in anticancer therapy.[6−12] In this context, it has been shown that ruthenium(II) complexes containing at least two highly π-deficient polyazaaromatic ligands such as 1,4,5,8-tetraazaphenanthrene (TAP) or 1,4,5,8,9,12-hexaazatriphenylene (HAT) are able to induce under illumination an electron-transfer process from a guanine residue of DNA to the excited complex.[13−16] This photoinduced electron transfer can give rise to the formation of a covalent adduct between the ruthenium(II) complex and the guanine base.[17,18] Despite these interesting photochemical properties, the high hydrophilicity of the nonderivatized ruthenium(II) complexes prevents their direct use in biological applications. Indeed, the photoreactive nonfunctionalized TAP metallic complexes are unable to penetrate the cell in order to reach the cytoplasm or nucleus. Interestingly, Puckett and Barton showed that complexes based on more hydrophobic ligands, such as the bathophenanthroline (DIP; 2,7-diphenyl-1,10-phenanthroline), can easily penetrate the cell membranes.[19] In our case, the use of more lipophilic ligands, such as DIP, is not relevant if the targeted complexes have to keep the capacity of photoanchoring to guanine bases.[17,18] Therefore, at least two TAP or HAT ligands are a prerequisite for design of the ruthenium compounds. Moreover, the penetration pathway of DIP complexes seems to correspond to passive diffusion, an unspecific mode of cellular vectorization. Another strategy consists of functionalizing a ligand for tethering the resulting complex on a vector to allow for cellular uptake.[20] By a relevant choice of the entities conjugated to the complex, a specific cell targeting could be obtained. In this context, we have recently developed a new photooxidizing Ru-TAP complex $[Ru(TAP)_2pytz]^{2+}$ with a ligand [pytz = 2-(1,2,3-triazol-4-yl)pyridine] that can be readily functionalized.[21]

An interesting approach consists of grafting these photoreactive ruthenium(II) complexes on calixarene derivatives,[22,23] which could combine an improvement of the cellular uptake with a specificity for cell receptor models thanks to multivalent recognition. Indeed, the hydrophobic calixarenes can constitute valuable molecular platforms for the design of ruthenium(II) complexes displaying particular cell penetration properties for specific cells. Recently, remarkable applications of calixarenes in biomedical science have been found; notably calixarene derivatives displaying antibacterial, antiviral, and anticancer

Received: June 10, 2013
Published: September 6, 2013

   dx.doi.org/10.1021/ic401468t | *Inorg. Chem.* 2013, 52, 11228−11236

properties have been described.[24] Interestingly, calixarenes can also behave as multivalent platforms[25,26] for example, by derivatization with carbohydrate functionalities in order to introduce recognition elements by the cell membranes.[27] It is well-known that multivalent systems can lead to strong binding with a biological target thanks to multiple simultaneous interactions.[28]

In this context, it was decided to functionalize calixarenes with a photoreactive $[Ru(TAP)_2]^{2+}$ motif. Different strategies were simultaneously investigated. Ruthenium(II) complexes tethered to both calix[4 or 6]arenes were envisioned for a comparison of the two platforms. Indeed, the large calix[6]-arene, on the one hand, has more derivatizable phenolic groups and thus is a priori more appropriate for the elaboration of multivalent systems, but, on the other hand, this oligomer is highly flexible and its selective functionalization is more difficult than that of calix[4]arene. For the introduction of recognition antenna like glycosides, the introduction of azido arms was envisaged because they could easily react with glycosides bearing an alkyne group through a 1,3-dipolar Huisgen cycloaddition. Finally, the comparison of behavior between the photoreactive $[Ru(TAP)_2phen]^{2+}$ and $[Ru(TAP)_2pytz]^{2+}$ motifs was also essential to test whether pytz could be chosen as a third ligand because it is more easily accessible.

In this work, we thus report the first studies of the electrochemical and photophysical properties of these different compounds that should allow selection of the best and most interesting calixarene-based Ru-TAP complexes for biological applications.

EXPERIMENTAL SECTION

Instrumentation. For the details concerning NMR, absorption, emission, and transient spectroscopy, see the Supporting Information.

Chemicals. All of the reactions were performed under an inert atmosphere. Anhydrous *N*,*N*-dimethylformamide (DMF) was obtained from Alfa Aesar. Anhydrous tetrahydrofuran (THF) was obtained from distillation on sodium/benzophenone. Anhydrous acetonitrile was distilled from CaH_2. All of the solvents and reagents for the syntheses were at least reagent grade quality and were used without further purification. The reaction mixtures from complexation with ruthenium(II) were protected from direct light during the synthesis to prevent photochemical degradation. Silica gel (230−400 mesh) was used for flash chromatography (FC). Neutral aluminum oxide was used for chromatography. The solvents for photophysical measurements were of spectroscopic grade. $Ru(phen)_2Cl_2$ (**21**) and $[Ru(TAP)_2(H_2O)_2]^{2+}(NO_3^-)_2$ (**22**) were prepared following the procedures described in the literature for the bipyridine (bpy) and phenanthroline (phen) complexes.[29,30] The syntheses of intermediate compounds **5**, **11**, **12**, **17**, **18**, and **23** are described in the Supporting Information. Because of the chirality of compounds **6**, **7**, **13**, **14**, and **19**, their ^{13}C NMR spectra (75 MHz, $CDCl_3$, 298 K) were too complicated for their interpretation.

Caution! *Although we have not encountered any problem, it is noted that small azide derivatives are potentially explosive and should be handled with appropriate precautions.*[31]

Synthesis of $[Ru(phen)_2phen'(C4)]^{2+}$ $(Cl^-)_2$ (6). Calix[4]-monoamidephenanthroline (**5**; 0.017 g, 0.0179 mmol, 1 equiv) was dissolved in DMF (1 mL), and **21** (0.013 g, 0.0244 mmol, 1.5 equiv) was added. The reaction mixture was stirred for 14 h at 100 °C under an inert atmosphere to yield a dark-red solution, which turned to brownish-orange. The reaction mixture was concentrated under reduced pressure, and the crude residue was purified by FC (8:2 CH_2Cl_2/MeOH) to yield the ruthenium complex **6** as an orange solid (0.017 g, 0.0113 mmol, 71%). R_f = 0.27 (8:2 CH_2Cl_2/MeOH). Mp: 283 °C (dec). IR: ν 3352, 2925, 1691, 1466, 1219 cm^{-1}. ^1H NMR (300 MHz, $CDCl_3$, 298 K): δ 1.18 (s, 9H, *t*Bu), 1.20 (s, 9H, *t*Bu), 1.21 (s, 9H, *t*Bu), 1.23 (s, 9H, *t*Bu), 3.33−3.48 (m, 4H, $ArCH_{2eq}$), 4.17−4.24 (m, 2H, $ArCH_{2ax}$), 4.38−4.42 (m, 2H, $ArCH_{2ax}$), 4.72−4.76 (m, 4H, NCH_2 + OCH_2), 6.94 (d, ^4J = 2.1 Hz, 1H, ArH), 6.98 (d,^4J = 2.1 Hz, 1H, ArH), 7.04−7.07 (m, 6H, ArH), 7.59−7.85 (m, 4H, H_{phen}), 7.87−8.00 (m, 2H, H_{phen}), 8.03−8.24 (m, 8H, H_{phen}), 8.36 (d, ^3J = 3.9 Hz, 1H, H_{phen}), 8.47−8.67 (m, 5H, H_{phen}), 9.37−9.60 (m, 3H, H_{phen} + OH), 9.71 (t, ^3J = 5.1 Hz, 1H, NH_{amide}), 10.20 (s_b, 1H, OH), 11.70 (s, 1H, NH_{phen}). HRMS (ESI-TOF). Calcd for $C_{84}H_{84}N_8O_6Ru$ (M^{2+}): *m*/*z* 698.2895. Found: *m*/*z* 698.2795.

Synthesis of $[Ru(TAP)_2phen'(C4)]^{2+}(NO_3^-)_2$ (7). **5** (0.051 g, 0.0542 mmol, 1 equiv) was dissolved in DMF (2 mL), and **22** (0.042 g, 0.0672 mmol, 1.3 equiv) was added. The reaction mixture was stirred for 14 h at 100 °C under an inert atmosphere to yield a dark-red solution, which turned to brownish-orange. The reaction mixture was concentrated under reduced pressure, and the crude residue was purified by neutral alumina chromatography (9:1 CH_2Cl_2/MeOH) to yield the ruthenium complex **7** as an orange solid (0.041 g, 0.0281 mmol, 52%). R_f = 0.39 (9:1 CH_2Cl_2/MeOH). Mp: 268 °C (dec). IR: ν 3377, 2964, 1681, 1482, 1275, 1106 cm^{-1}. ^1H NMR (300 MHz, CD_3OD, 298 K): δ 1.13 (s, 9H, *t*Bu), 1.17 (s, 9H, *t*Bu), 1.20 (s, 9H, *t*Bu), 1.21 (s, 9H, *t*Bu), 3.01 (d, ^2J = 12.6 Hz, 1H, $ArCH_{2eq}$), 3.23 (d, ^2J = 12.6 Hz, 1H, $ArCH_{2eq}$), 3.34−3.36 (m, 2H, $ArCH_{2eq}$), 4.12 (d, ^2J = 12.6 Hz, 1H, $ArCH_{2ax}$), 4.29 (d, ^2J = 12.6 Hz, 1H, $ArCH_{2ax}$), 4.48−4.52 (m, 2H, $ArCH_{2ax}$), 4.58−4.60 (m, 4H, NCH_2 + OCH_2), 6.80 (d, ^4J = 2.1 Hz, 1H, ArH), 6.92 (d, ^4J = 2.4 Hz, 1H, ArH), 6.97 (d, ^4J = 2.7 Hz, 1H, ArH), 6.99 (d, ^4J = 2.4 Hz, 1H, ArH), 7.05−7.08 (m, 2H, ArH), 7.13 (d, ^4J = 2.4 Hz, 1H, ArH), 7.17 (d, ^4J = 2.7 Hz, 1H, ArH), 7.64 (dd, ^3J = 5.4 Hz, ^3J = 8.7 Hz, 1H, H_{phen}), 7.78 (dd, ^3J = 5.4 Hz, ^3J = 8.7 Hz, 1H, H_{phen}), 8.17−8.22 (m, 2H, H_{phen}), 8.24 (d, ^3J = 3.0 Hz, 1H, H_{TAP}), 8.30 (d, ^3J = 2.7 Hz, 1H, H_{TAP}), 8.39−8.42 (m, 2H, H_{phen}), 8.51 (s, 1H, H_{phen}), 8.59−8.70 (m, 5H, $H_{phen/TAP}$), 8.92 (d, ^3J = 8.4 Hz, 1H, H_{phen}), 8.96−9.06 (m, 4H, H_{TAP}). HRMS (ESI-TOF). Calcd for $C_{80}H_{80}N_{12}O_6Ru$ (M^{2+}): *m*/*z* 700.7717. Found: *m*/*z* 700.7702.

Synthesis of $[Ru(phen)_2phen'(C6)]^{2+}$ $(Cl^-)_2$ (13). Calix[6]-monoamidephenanthroline (**12**; 0.052 g, 0.0401 mmol, 1 equiv) was dissolved in DMF (2 mL), and **21** (0.041 g, 0.0778 mmol, 2 equiv) was added. The reaction mixture was stirred for 14 h at 100 °C under an inert atmosphere to yield a dark-red solution, which turned to brownish-orange. The reaction mixture was concentrated under reduced pressure, and the crude residue was purified by neutral alumina chromatography (9:1 CH_2Cl_2/MeOH) to yield the ruthenium complex **13** as an orange solid (0.025 g, 0.0141 mmol, 35%). R_f = 0.36 (9:1 CH_2Cl_2/MeOH). Mp: 185−186 °C. IR: ν 3417, 2959, 1685, 1483, 1206 cm^{-1}. ^1H NMR (300 MHz, $CDCl_3$, 298 K): δ 0.79 (s, 9H, *t*Bu), 0.83 (s, 9H, *t*Bu), 1.09 (s, 9H, *t*Bu), 1.17−1.18 (m, 18H, *t*Bu), 1.22 (s, 9H, *t*Bu), 3.02 (s, 3H, OMe), 3.22−3.33 (m, 4H, OMe + $ArCH_{2eq}$), 3.36−3.55 (m, 8H, OMe + $ArCH_{2eq}$), 3.87 (d, ^2J = 13.8 Hz, 1H, $ArCH_{2ax}$), 4.05−4.13 (m, 2H, $ArCH_{2ax}$), 4.21 (d, ^2J = 16.2 Hz, 1H, $ArCH_{2ax}$), 4.34 (s_b, 2H, OCH_2), 4.36−4.41 (m, 2H, $ArCH_{2ax}$), 4.56 (s_b, 2H, NCH_2), 6.65−6.66 (m, 2H, ArH), 6.75 (s, 1H, ArH), 6.79 (s, 1H, ArH), 6.82 (s, 1H, ArH), 6.91−6.95 (m, 4H, ArH), 6.99 (s, 1H, ArH), 7.13−7.14 (m, 2H, ArH), 7.59−7.75 (m, 5H, H_{phen}), 7.84 (s_b, 1H, NH_{amide}), 7.89−7.97 (m, 2H, H_{phen}), 8.05−8.31 (m, 9H, H_{phen}), 8.37−8.60 (m, 8H, H_{phen} + OH), 9.18 (d, ^3J = 6.3 Hz, 1H, H_{phen}), 11.14 (s_b, 1H, NH_{phen}). HRMS (ESI-TOF). Calcd for $C_{109}H_{118}N_8O_8Ru$ (M^{2+}): *m*/*z* 881.9091. Found: *m*/*z* 881.9075.

Synthesis of $[Ru(TAP)_2phen'(C6)]^{2+}(NO_3^-)_2$ (14). **12** (0.041 g, 0.0314 mmol, 1 equiv) was dissolved in DMF (2 mL), and **22** (0.031 g, 0.0496 mmol, 1.6 equiv) was added. The reaction mixture was stirred for 14 h at 100 °C under an inert atmosphere to yield a dark-red solution, which turned to brownish-orange. The reaction mixture was concentrated under reduced pressure, and the crude residue was purified by neutral alumina chromatography (9:1 CH_2Cl_2/MeOH) to yield the ruthenium complex **14** as an orange solid (0.030 g, 0.0178 mmol, 50%). R_f = 0.39 (9:1 CH_2Cl_2/MeOH). Mp: 210−212 °C (dec). IR: ν 3454, 2931, 1673, 1483 cm^{-1}. ^1H NMR (300 MHz, $CDCl_3$, 298 K): δ 0.74 (s, 9H, *t*Bu), 0.82 (s, 9H, *t*Bu), 1.11 (s, 9H, *t*Bu), 1.15 (s, 9H, *t*Bu), 1.16 (s, 9H, *t*Bu), 1.29 (s, 9H, *t*Bu), 2.85 (s, 3H, OMe), 2.95 (d, ^2J = 14.7 Hz, 1H, $ArCH_{2eq}$), 3.16−3.33 (m, 4H, OMe + $ArCH_{2eq}$), 3.46−3.57 (m, 4H, $ArCH_{2eq}$), 3.60 (s, 3H, OMe), 3.68 (d, ^2J = 14.7

dx.doi.org/10.1021/ic401468t | *Inorg. Chem.* 2013, 52, 11228−11236

Scheme 1. Syntheses of Calixarene-based Ruthenium(II) Complexes 6, 7, 13, 14, and 19

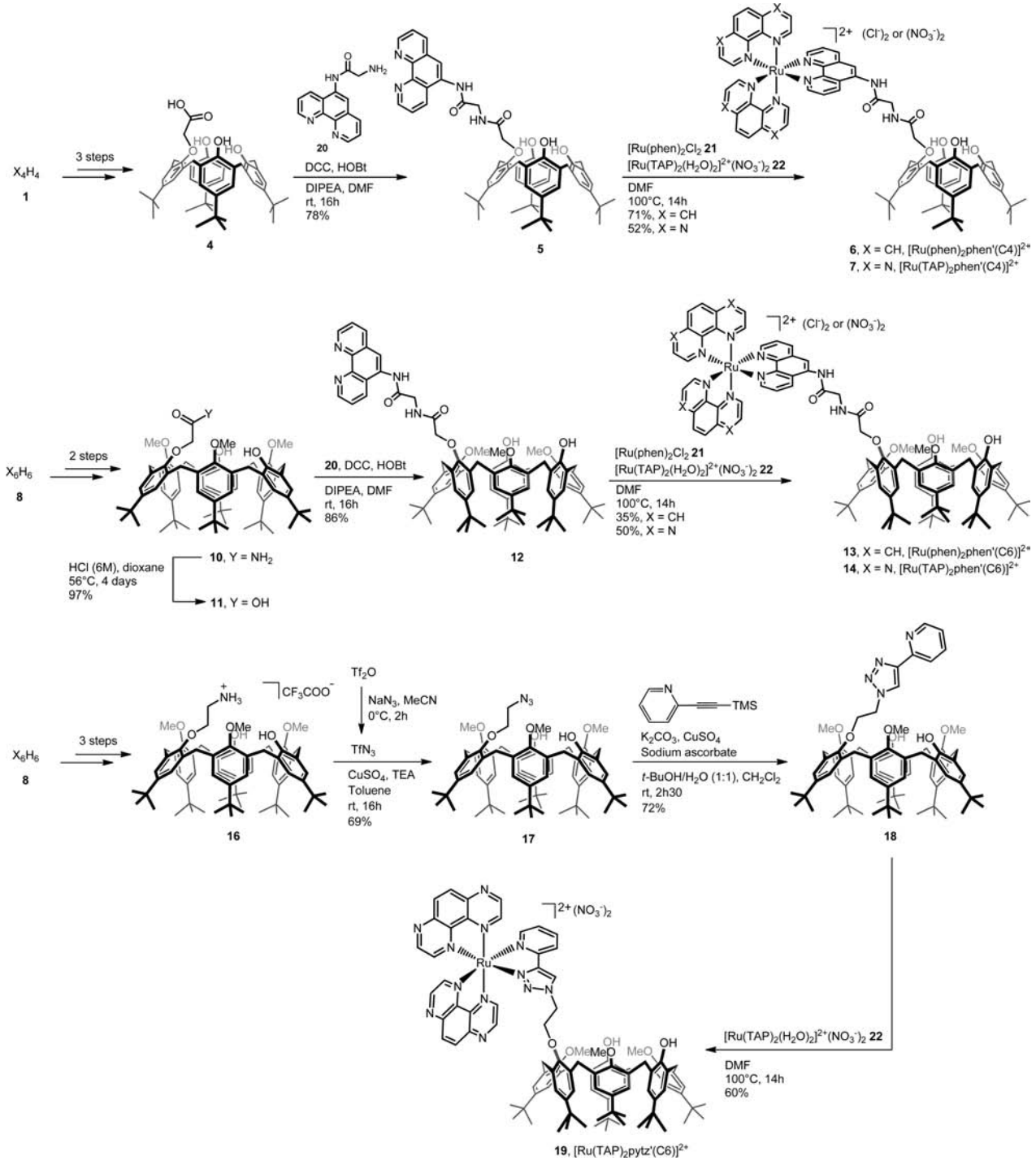

Hz, 1H, $ArCH_{2ax}$), 4.00 (d, ^2J = 12.3 Hz, 1H, $ArCH_{2ax}$), 4.11−4.22 (m, 3H, $ArCH_{2ax}$ + OCH_2), 4.35−4.39 (m, 5H, $ArCH_{2ax}$ + NCH_2), 6.59 (s, 1H, ArH), 6.63 (s, 1H, ArH), 6.66 (s, 1H, ArH), 6.86 (s, 1H, ArH), 6.89 (s, 1H, ArH), 6.93 (s, 1H, ArH), 6.97 (s, 1H, ArH), 7.00 (s, 1H, ArH), 7.04 (s, 1H, ArH), 7.10 (s, 1H, ArH), 7.21 (s, 2H, ArH), 7.67 (mult, 1H, H_{phen}), 7.77−7.82 (m, 2H, H_{phen} + NH_{amide}), 7.97 (d, ^3J = 7.2 Hz, 1H, H_{phen}), 8.36 (s, 1H, H_{phen}), 8.43 (d, ^3J = 6.6 Hz, 1H, H_{phen}), 8.46−8.69 (m, 8H, $H_{phen/TAP}$), 8.78 (s, 1H, H_{TAP}), 8.87−9.02 (m, 4H, $H_{phen/TAP}$ + OH), 9.06−9.17 (m, 3H, H_{TAP}), 10.37 (s_b, 1H, NH_{phen}). HRMS (ESI-TOF). Calcd for $C_{105}H_{114}N_{12}O_8Ru$: m/z 886.8980. Found: m/z 886.8988.

Synthesis of $[Ru(TAP)_2pytz'(C6)]^{2+}(NO_3^-)_2$ (19). Calix[6]mono-2-(1,2,3-triazol-4-yl)pyridine (**18**; 0.040 g, 0.0337 mmol, 1 equiv) was dissolved in DMF (2 mL), and **22** (0.030 g, 0.0480 mmol, 1.4 equiv) was added. The reaction mixture was stirred at 100 °C for 14 h to yield a dark-red solution, which turned to brownish-orange. The reaction mixture was concentrated under reduced pressure, and the crude residue was purified by neutral alumina chromatography (9:1 CH_2Cl_2/MeOH) to yield the ruthenium complex **19** as an orange solid (0.033 g, 0.0199 mmol, 60%). R_f = 0.32 (9:1 CH_2Cl_2/MeOH). Mp: 265−267 °C (dec). IR: ν 3395, 2962, 1484, 1367, 1211 cm^{-1}. ^1H NMR (400 MHz, $CDCl_3$, 328 K): δ 0.72 (s_b, 9H, *t*Bu), 0.91 (s, 9H, *t*Bu), 0.94 (s, 9H, *t*Bu), 1.21 (s, 9H, *t*Bu), 1.23 (s, 9H, *t*Bu), 1.43 (s, 9H, *t*Bu), 2.55 (s_b, 2H, OCH_2), 3.05 (s, 3H, OMe), 3.21 (d, ^2J = 16.0 Hz, 1H, $ArCH_{2eq}$), 3.26 (d, ^2J = 15.2 Hz, 1H, $ArCH_{2eq}$), 3.32−3.40 (m, 3H, $ArCH_{2eq}$), 3.47−3.55 (m, 3H, $ArCH_{2ax}$ + $ArCH_{2eq}$), 3.61−3.69 (m,

dx.doi.org/10.1021/ic401468t | *Inorg. Chem.* 2013, 52, 11228−11236

Scheme 2. Synthesis of the Calixarene-Based Ruthenium(II) Complex 24

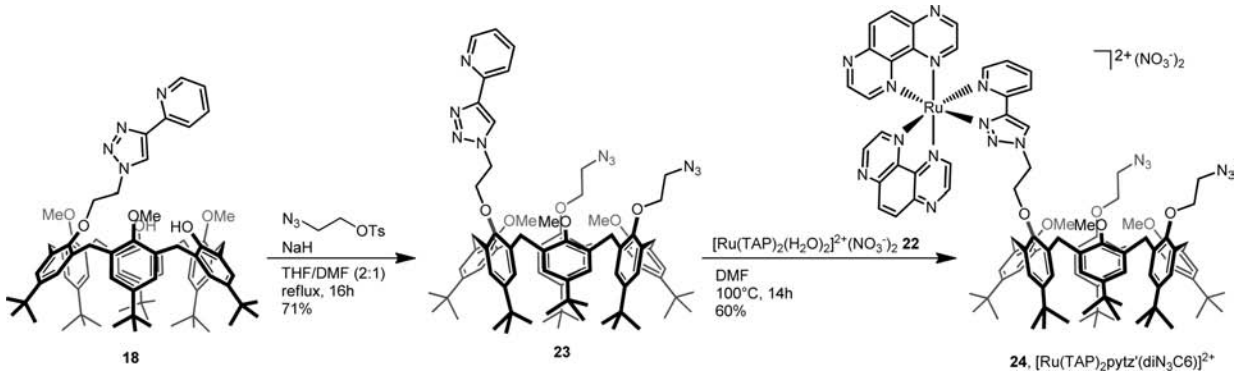

Table 1. Electrochemical Data for Complexes 7, 14, 19, and 24 and Reference Complexes[a]

complex	oxidation (V vs SCE)	reduction (V vs SCE)	E^*_{red}[b] (V vs SCE)
$[Ru(TAP)_2phen]^{2+}(Cl^-)_2$ (**25**)[39]	+1.73	−0.83 (r, T), −1.01 (r, T), −1.55 (r, P), −1.74 (r, T)	+1.17
$[Ru(TAP)_2pytz]^{2+}(NO_3^-)_2$ (**26**)[21]	+1.78	−0.78 (r, T), −0.97 (r, T), −1.50 (r, T), −1.75 (r, T, or pytz)	+1.23
$[Ru(TAP)_2phen'(C4)]^{2+}(NO_3^-)_2$ (**7**)	+1.78	−0.77 (r, T), −0.99 (r, T), −1.37	+1.21
$[Ru(TAP)_2phen'(C6)]^{2+}(NO_3^-)_2$ (**14**)	+1.76	−0.75 (r, T), −1.00 (r, T), −1.38	+1.23
$[Ru(TAP)_2pytz'(C6)]^{2+}(NO_3^-)_2$ (**19**)	+1.79	−0.78 (r, T), −0.98 (r, T), −1.37, −1.68	+1.23
$[Ru(TAP)_2pytz'(diN_3C6)]^{2+}(NO_3^-)_2$ (**24**)	+1.79	−0.67 (N_3 + T)[c], −0.99 (r, T)	+1.33[c]

[a]Redox potentials measured by cyclic voltammetry in dry deoxygenated MeCN, V versus SCE, at room temperature, with 0.1 M $Bu_4N^+PF_6^-$ as the supporting electrolyte and a platinum working electrode. The reversibility and attribution of the waves are given in parentheses. r = reversible; T = 1,4,5,8-tetraazaphenanthrene; P = 1,10-phenanthroline. [b]The corresponding reduction potentials in the excited state (vs SCE), as estimated from the reduction potential in the ground state and the energy of the emission maximum in MeCN ($E_{red}^* \approx E_{red} + \Delta E_{\lambda_{max}}$). [c]Approximate value for **24** because of overlapping of the reduction waves (Figure S53 in the Supporting Information).

8H, OMe + NCH_2), 3.96 (d, ^2J = 16.0 Hz, 1H, $ArCH_{2ax}$), 4.03 (d, ^2J = 15.2 Hz, 1H, $ArCH_{2ax}$), 4.09 (d, ^2J = 14.8 Hz, 1H, $ArCH_{2ax}$), 4.15 (d, ^2J = 14.8 Hz, 1H, $ArCH_{2ax}$), 6.30 (s, 1H, ArH), 6.36 (s, 1H, ArH), 6.65 (s, 1H, ArH), 6.74 (s, 1H, ArH), 6.82−6.86 (m, 5H, ArH), 7.11−7.13 (m, 2H, ArH), 7.28 (d, ^4J = 2.4 Hz, 1H, ArH), 7.44 (t, ^3J = 6.4 Hz, 1H, H_{py}), 7.96 (d, ^3J = 5.6 Hz, 1H, H_{py}), 8.01−8.08 (m, 2H, H_{TAP} + H_{py}), 8.24 (d, ^3J = 9.2 Hz, 1H, H_{TAP}), 8.37 (d, ^3J = 7.2 Hz, 1H, H_{py}), 8.52−8.59 (m, 3H, H_{TAP}), 8.70−8.76 (m, 2H, H_{TAP}), 9.00 (d, ^4J = 2.4 Hz, 2H, H_{TAP}), 9.09−9.17 (m, 5H, H_{TAP} + OH), 9.25 (s_b, 1H, H_{tz}). HRMS (ESI-TOF). Calcd for $C_{98}H_{110}N_{12}O_6Ru$ (M^{2+}): m/z 823.8891. Found: m/z 823.8884.

Synthesis of $[Ru(TAP)_2pytz'(diN_3C6)]^{2+}(NO_3^-)_2$ (24). Calix[6]-diazidomono-2-(1,2,3-triazol-4-yl)pyridine (**23**; 0.060 g, 0.0452 mmol, 1 equiv) was dissolved in DMF (2.5 mL), and **22** (0.044 g, 0.0704 mmol, 1.6 equiv) was added. The reaction mixture was stirred for 14 h at 100 °C to yield a dark-red solution, which turned to brownish-orange. The reaction mixture was concentrated under reduced pressure, and the crude residue was purified by neutral alumina preparative plate (9:1 CH_2Cl_2/MeOH) to yield the ruthenium complex **24** as an orange solid (0.052 g, 0.0270 mmol, 60%). R_f = 0.38 (9:1 CH_2Cl_2/MeOH). Mp: 251−253 °C (dec). IR: ν 3449, 2964, 2112, 1480, 1364, 1204 cm^{-1}. ^1H NMR (400 MHz, CD_3OD, 298 K): δ 0.84−0.89 (m, 18H, *t*Bu), 0.98 (s, 9H, *t*Bu), 1.33 (s, 9H, *t*Bu), 1.36 (s, 9H, *t*Bu), 1.37 (s, 9H, *t*Bu), 2.41 (s_b, 3H, OMe), 2.48 (s_b, 3H, OMe), 2.64 (s_b, 3H, OMe), 3.22 (d, ^2J = 14.8 Hz, 1H, $ArCH_{2eq}$), 3.42 (d, ^2J = 14.4 Hz, 1H, $ArCH_{2eq}$), 3.46−3.62 (m, 8H, $ArCH_{2eq}$ + CH_2N_3), 3.82−4.07 (m, 7H, OCH_2 + $ArCH_{2ax}$), 4.16 (d, ^2J = 14.4 Hz, 1H, $ArCH_{2ax}$), 4.28−4.53 (m, 4H, $ArCH_{2ax}$), 4.71−4.85 (s_b, 2H, CH_2N), 6.71−6.80 (m, 4H, ArH), 6.88−6.92 (m, 2H, ArH), 7.24−7.33 (m, 6H, ArH), 7.43 (t, ^3J = 6.4 Hz, 1H, H_{py}), 7.80 (d, ^3J = 5.6 Hz, 1H, H_{py}), 8.26 (t, ^3J = 7.2 Hz, 1H, H_{py}), 8.32 (d, ^4J = 2.8 Hz, 1H, H_{TAP}), 8.42 (d, ^4J = 2.4 Hz, 1H, H_{TAP}), 8.46−8.48 (m, 3H, H_{py} + H_{TAP}), 8.52−8.60 (m, 3H, H_{TAP}), 8.67 (s, 2H, H_{TAP}), 8.92 (d, ^4J = 2.4 Hz, 1H, H_{TAP}), 9.00−9.05 (m, 2H, H_{TAP}), 9.26 (s_b, 1H, H_{tz}). ^{13}C NMR (75 MHz, CD_3OD, 298 K): δ 29.9−30.8 (m), 31.8, 31.9, 32.0 (2C), 35.0(7), 35.1(8), 35.2(0), 35.2(4), 52.4, 54.2, 61.1, 61.2, 62.3, 72.5, 72.6, 124.6, 125.5−125.9, 128.0, 128.8−129.1, 133.8−134.9, 141.0, 143.6, 143.6(7), 143.6(9), 146.5, 146.7, 146.9, 147.0, 147.3(5), 147.4(4), 147.6, 147.7, 148.2, 149.2, 149.3, 150.2, 150.7, 150.8, 151.5, 151.6, 152.7, 153.9, 155.1, 155.2, 155.5. HRMS (ESI-TOF). Calcd for $C_{102}H_{117}N_{18}O_6Ru$ (M^{2+}): m/z 892.9218. Found: m/z 892.9196.

RESULTS

Syntheses. The syntheses of calixarene-based ruthenium(II) complexes required the selective linkage of one chelating phen or pytz unit on the narrow rim of calix[4 or 6]arene scaffolds. Several examples of monofunctionalization have already been reported in the literature on either calix[4 or 6]arenes.[32−35] Thus, known procedures were used for the preparation of precursors **4**,[36] **10**,[35] and **16**[34] from either X_4H_4 (**1**) or X_6H_6 (**8**; Scheme 1).

Hydrolysis of the amido group of **10** led to the calix[6]arene **11**. Afterward, the known aminophenanthroline **20**[37] was linked at the level of the carboxylate group of **4** and **11** through a peptide-type coupling reaction. The resulting calixarene-based ligands **5** and **12** were obtained in 78% and 86% yield, respectively, after FC purification on silica gel. Further reactions of ligands **5** and **12** with **21** and **22** in anhydrous DMF yielded the calixarene-based ruthenium(II) complexes **6**, **7**, **13**, and **14** in 71%, 52%, 35%, and 50% yield, respectively, either after FC purification on silica gel (in the case of **6**) or after chromatography on neutral alumina (in the cases of **7**, **13**, and **14**).

The ligand **18** was obtained in a two-step sequence from the calix[6]arene **16** monofunctionalized by an amino group. First, the reaction of **16** with TfN_3 (previously prepared from Tf_2O and NaN_3) in toluene in the presence of triethylamine and a catalytic amount of $CuSO_4$ led to the calix[6]arene **17** in 69% yield. The latter was then reacted with 2-(trimethylsilyl)-

dx.doi.org/10.1021/ic401468t | Inorg. Chem. 2013, 52, 11228−11236

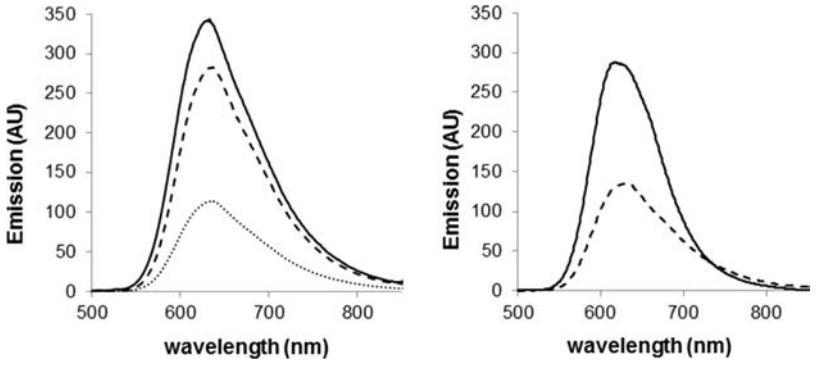

Figure 1. (left) Emission spectra (298 K, Ar) in MeCN for complexes **7** (dotted line), **14** (dashed line), and **25** (solid line). (right) Emission spectra (298 K, Ar) in MeCN for complexes **26** (solid line) and **19** (dashed line).

Table 2. Emission Data in Acetonitrile under Air and Argon at Room Temperature

A. For the Reference Complexes and Complex without Intramolecular Luminescence Quenching							
complex	λ_{max}, nm	τ_0(air),[b] ns	τ_0(Ar),[b] ns	$k_r + k_{nr}$, $\times 10^6$ s^{-1}	Φ(Ar),[a] $\times 10^{-3}$	k_r(Ar),[a] $\times 10^3$ s^{-1}	k_{nr}(Ar),[a] $\times 10^5$ s^{-1}
$[Ru(phen)_3]^{2+}(Cl^-)_2$ (**27**)[41]	604	120	460	2.17	28	61	21
$[Ru(phen)_2phen'(C4)]^{2+}(NO_3^-)_2$ (**6**)	600	129	515	1.94	28	54	19
$[Ru(phen)_2phen'(C6)]^{2+}(NO_3^-)_2$ (**13**)	600	129	461	2.16	27	59	21
$[Ru(TAP)_2phen]^{2+}(Cl^-)_2$ (**25**)[39]	626	760	1800	0.56	55	30	5
$[Ru(TAP)_2pytz]^{2+}(NO_3^-)_2$ (**26**)[21]	616	385	536	1.86	19	35	18
$[Ru(TAP)_2pytz'(diN_3C6)]^{2+}(NO_3^-)_2$ (**24**)	619	386	529	1.84	21	38	18
B. For the Complexes with Intramolecular Luminescence Quenching							
complex	λ_{max}, nm	τ_{av}(air),[c] ns	τ_1(Ar)/B_1, ns	τ_2(Ar)/B_2, ns	τ_3(Ar)/B_3, ns	τ_{av}(Ar),[c] ns	k_{qi}[d], $\times 10^6$ s^{-1}	Φ(Ar),[a] $\times 10^{-3}$
$[Ru(TAP)_2phen'(C4)]^{2+}(NO_3^-)_2$ (**7**)	630	256	12 (46%)	311 (14%)	1192 (40%)	529	1.34	14
$[Ru(TAP)_2phen'(C6)]^{2+}(NO_3^-)_2$ (**14**)	627	467	566 (58%)	1020 (42%)	-	756	0.77	21
$[Ru(TAP)_2pytz'(C6)]^{2+}(NO_3^-)_2$ (**19**)	619	330	272 (75%)	632 (25%)	-	426	0.48	11

[a]The luminescence quantum yields Φ (approximate error <20%) were determined from the Φ value of $[Ru(bpy)_3]^{2+}$ as a reference.[42] The radiative deactivation rate constant $k_r = \Phi/\tau$ and nonradiative deactivation rate constant $k_{nr} = (1/\tau) - k_r$. [b]The luminescence decays corresponding to the excited-state lifetimes (τ) were measured by SPC or pulsed laser. Estimated experimental errors for the lifetimes: ~10%. [c]Data processing exhibits two or three excited-state lifetimes with two or three different contributions (B in parentheses); the calculated average lifetimes correspond to $\tau_{average} = \tau_{av} = \sum_i \tau_i B_i/100$, under air and argon. [d]$k_{qi} = 1/\tau_{av} - 1/\tau_0$ under argon with τ_0 corresponding to the excited-state lifetime of the reference complexes **25** or **26** .

ethynylpyridine in *t*BuOH/H_2O/CH_2Cl_2 in the presence of K_2CO_3, sodium ascorbate, and a catalytic amount of $CuSO_4$. The presence of K_2CO_3 allowed *in situ* deprotection of the alkyne reactant. It is noteworthy to mention that a washing of crude **18** with an aqueous NH_4OH solution (5%) was necessary in order to remove the copper ion, which was likely complexed to the obtained ligand. Pure calixarene-based ligand **18** was obtained after FC purification on silica gel in 72% yield. The subsequent reaction of this ligand with **22** in anhydrous DMF led to the ruthenium(II) complex **19** in 60% yield after chromatography on neutral alumina.

The calix[6]arene **18** monofunctionalized by a pytz arm on the narrow rim was alkylated by 2-(azidoethyl)-4-methylbenzenesulfonate[38] in anhydrous THF/DMF to obtain the calixarene-based ligand **23** in 71% yield (Scheme 2). Finally, the reaction of **23** with **22** in anhydrous DMF led to the calixarene-based ruthenium(II) complex **24** in 60% yield after preparative chromatography on neutral alumina.

All of these complexes were obtained as orange solids and are soluble in polar (e.g., MeCN and MeOH) and nonpolar (e.g., CH_2Cl_2 and $CHCl_3$) organic solvents.

Electrochemical Data. The electrochemical data for complexes **7**, **14**, **19**, and **24** bearing two TAP ligands, along with those for reference complexes **25** and **26**, are collected in Table 1. phen′ and pytz′ stand for the ligands attached by their linker to calixarene.

The four TAP complexes **7**, **14**, **19**, and **24** exhibit an oxidation wave at potentials 1.76−1.79 V vs SCE, which correspond to oxidation of the ruthenium(II) center. Compared to the untethered reference complex **25**, the corresponding complexes **7** and **14** with a phen−calixarene exhibit an oxidation potential value slightly more positive probably because of the influence of the amido spacer. In reduction, complexes **7**, **14**, and **19** present two first reversible waves that can be attributed to the reduction of the two TAP ligands in comparison with the reference complexes **25** and **26**. The third wave around −1.37 V vs SCE, can be assigned for complexes **7** and **14** to the first reduction of a phen ligand and for complex **19** probably to a second reduction of one TAP ligand. Complex **24** exhibits two reduction waves at −0.67 and −0.99 V vs SCE also attributed to each TAP reduction but with an intensity more important for the first wave. This could correspond to an overlapping of the reduction of the azido groups with the first reduction of a first TAP ligand (Figure S53 in the Supporting Information).

All of these data show that the calixarene platform does not affect much the electrochemical properties of the tethered ruthenium(II) complexes.

dx.doi.org/10.1021/ic401468t | *Inorg. Chem.* 2013, 52, 11228−11236

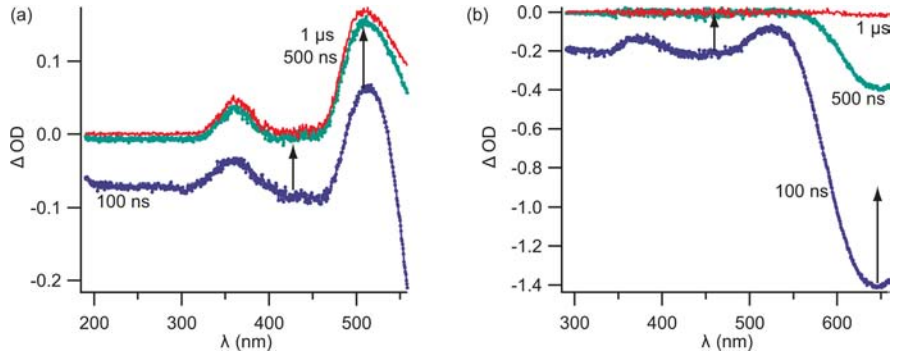

Figure 2. Differential TA for **25** in the presence of (a) 45 mM PhOH or (b) 1.25 mM PTSA, in argon-saturated acetonitrile, recorded 100 ns, 500 ns, and 1 μs after the laser pulse.

Absorption, Emission, Luminescence Lifetimes and Related Rate Constants. The absorption spectra were recorded in acetonitrile at room temperature for all of the ruthenium(II) calixarene complexes (Figure S57 in the Supporting Information). The most bathochromic absorption bands around 450−460 nm correspond to $d\pi(Ru)-\pi^*$(phen/TAP) MLCT transitions like those for the untethered reference complexes. The emissions originate from the ^{3}MLCT states and are given in Figure 1, with λ_{max} values collected in Table 2. The oxidizing powers of the excited states have been estimated from the emission maxima and reduction potentials of the first reduction waves (Table 1). It is noteworthy that they are similar to those of the reference complexes.[40]

In the case of the TAP-based complexes **7**, **14**, and **19**, although the emission maxima (λ_{max}) of these calixarene-based ruthenium(II) complexes are similar to those of the reference complexes **25** and **26**, the luminescence intensities are influenced by the presence of the calixarene platform (Figure 1). The corresponding quantum yields of emission [Φ(Ar)] and luminescence lifetimes (τ) are gathered in Table 2B. Under pulsed illumination of the three complexes **7**, **14**, and **19**, the luminescence decays do not correspond to single exponentials and bi- or triexponential functions have to be used. Therefore, we also calculated average emission lifetimes (τ_{av}) under air and argon (Table 2B). These values are shorter than those of the reference complexes **25** and **26** (Table 2A), indicating an intramolecular quenching of the tethered excited ruthenium complexes by the calixarene. This shortening of the lifetime is in agreement with lower emission intensities (Figure 1) and smaller values of Φ emission for the tethered complexes compared to those of the reference compounds [cf. Φ(Ar) in Table 2A,B]. The intramolecular luminescence quenching (k_{qi}) for each of the complexes **7**, **14**, and **19** (Table 2B) was roughly evaluated by using a τ_0 value of the corresponding free complex (Table 2A). Because the quenching cannot be assigned to an energy transfer, based on the respective absorption spectra of the calixarene platform and ruthenium complexes, it could be attributed to an intramolecular electron transfer (ET) or an intramolecular proton transfer (HT)[43,44] or both ET and HT (thus, a proton-coupled electron transfer, PCET) from the phenolic groups of the calixarenes to the excited state of the Ru^{II}(TAP) complexes.[45]

In contrast, for **6** and **13** (Table 2A), the fitting of luminescence decay corresponds to a single exponential with a luminescence lifetime similar to that of the reference complex $[Ru(phen)_3]^{2+}$ (**27**; Table 2A). Thus, for **6** and **13**, no luminescence quenching is observed, which is confirmed by the quantum yield values [Φ(Ar); Table 2A]. Therefore, for the calixarene-based complexes **6** and **13**, the associated deactivation rate constants k_r and k_{nr} could be calculated and are quite similar to the values for **27**. This absence of quenching can be attributed to the inability of phen-based complexes to undergo an ET or HT process in their excited state.

For the reasons explained in the Introduction, we also examined the luminescence properties of the azido-derivatized calixarene platform **24**. In that case too, no luminescence quenching is observed (Table 2A). Indeed, the luminescence lifetime [τ_0(Ar)], the corresponding quantum yield of emission [Φ(Ar)], and the radiative (k_r) and nonradiative (k_{nr}) rate constants are similar to those of the reference complex **26** (Table 2A).

All of these photophysical results indicate thus that the phenolic groups of the calixarene skeleton are responsible for luminescence quenching with TAP complexes (**7**, **14**, and **19**).

Type of Quenching Process. The Case of Free 25. In order to determine whether the emission quenching results from an ET or HT or both for compounds **7**, **14**, and **19**, we examined the behavior of **25** in acetonitrile, in the presence of phenol (PhOH) or an acid (*p*-toluenesulfonic acid, PTSA), by Stern−Volmer experiments of the luminescence intensities and lifetimes (Figures S58−S59 in the Supporting Information). Both types of experiments lead to linear plots. With phenol, the quenching rate constant is $k_q = 9.2 \times 10^7$ M^{-1} s^{-1}, suggesting that the quenching process is not diffusion-controlled. The quenching of excited **25** by PTSA yields a k_q value of 4.8×10^9 M^{-1} s^{-1}, indicating that the quenching, due in this case to proton transfer, is diffusion-controlled.

In order to evaluate the characteristics of phenol quenching compared to proton quenching, nanosecond transient absorption (TA) under pulsed illumination were performed in acetonitrile with phenol or PTSA. In the presence of 45 mM PhOH or 1.25 mM PTSA, the TA data show a clear difference between the behaviors of TA due to the two types of quenching agents.

In the presence of phenol, a positive TA of around 510 nm is still detected after 1 μs (Figure 2a), whereas with PTSA, after such a long time, a TA is no longer detected (Figure 2b). With PTSA, in the shorter time scale (100−500 ns), only depletion and recovery of the ground state can be observed in the 400−500 nm spectral region as well as extinction of the emission at λ > 600 nm, with a lifetime characteristic of the excited complex with 1.25 mM PTSA (τ = 150 ns). With phenol, the absorption around 510 nm after 1 μs can be assigned to the reduced complex, protonated or nonprotonated form.[46] Luminescence

dx.doi.org/10.1021/ic401468t | *Inorg. Chem.* 2013, 52, 11228−11236

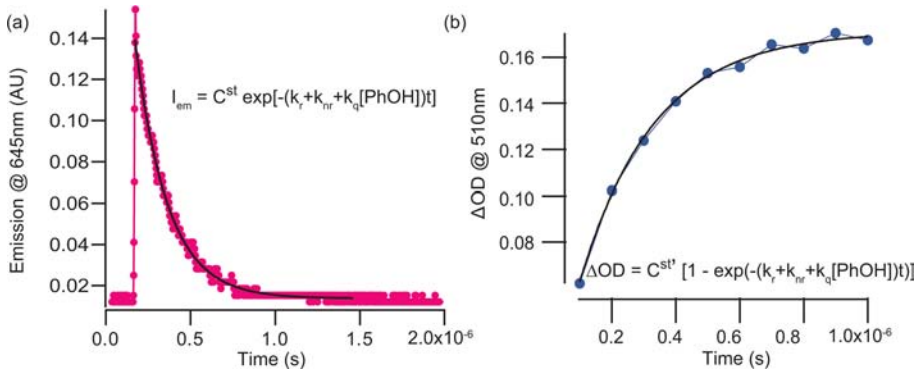

Figure 3. 25 in deoxygenated acetonitrile with 45 mM PhOH: (a) decay of the emission signal at 645 nm corresponding to luminescence at λ = 650 nm; (b) appearance of TA at 510 nm for the same sample.

quenching induced by phenol can thus be attributed to an ET (which could be coupled to a HT). In order to further characterize this TA, kinetic analyses have been performed in the nanosecond and microsecond time domains, in the presence of 45 mM PhOH (Figures 3 and 4). The TA at

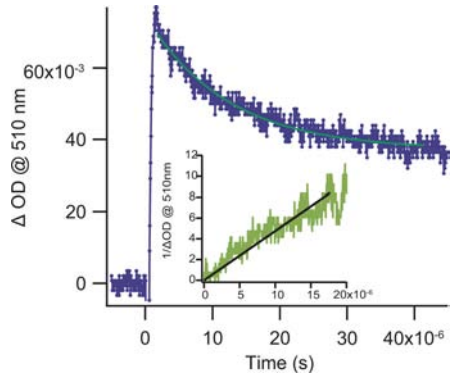

Figure 4. 25 in deoxygenated acetonitrile with 45 mM PhOH. Decay of the TA at 510 nm in a few tens of microseconds. No baseline recovery. Inset: Kinetic treatment according to a bimolecular equimolecular process, thus with 1/ΔOD plotted as a function of time.

510 nm appears in the same time domain (Figure 3b) as the emission decay (Figure 3a). The emission should decay with the same rate constant ($k_{em} = k_r + k_{nr} + k_q[PhOH]$) as that corresponding to the appearance of a reduced complex. This is indeed the case because treatment of the curve in Figure 3b according to equation $\Delta OD = \text{constant}(1 - \exp(k_r + k_{nr} + kq[PhOH]t)$ gives a value for $k_r + k_{nr} + kq[PhOH] = 4.3 \times 10^6$ s^{-1}, which corresponds within experimental error to the inverse of the emission lifetime in the presence of 45 mM PhOH (1/200 ns = 5×10^6 s^{-1}). The quenching process can thus be attributed to reduction of the excited complex with a rather low rate constant k_q (9.2×10^7 M^{-1} s^{-1} determined from the Stern–Volmer plot). This suggests that the ET process is not very exergonic.

In the longer time scale, the TA at 510 nm decays in a 30 μs time range (Figure 4) according to a bimolecular equimolecular process, at least until 20 μs, and without baseline recovery. This TA behavior is also in agreement with an ET process (see the Discussion and Conclusion section).

With TAP complexes, such a photoinduced ET could be coupled with proton transfer because of the presence of nonchelated nitrogen atoms that can be protonated or form hydrogen-bonding interactions.[46] Therefore, we also measured the k_q value with deuterated phenol (PhOD; Figure S61 in the Supporting Information); in that case, $k_q(D) = 7.3 \times 10^7$ M^{-1} s^{-1}. This gives an isotopic effect of $k_q(H)/k_q(D) = 1.26$, which would indicate that the process is proton-coupled.

Quenching Process in the Calixarene-Based Ru^{II}(TAP) Complexes. On the basis of the behavior of the free excited complex with phenol, we can conclude by extrapolation that the quenching in the calixarene-based Ru^{II}(TAP) complexes takes place by ET.[47] We tried to record TA with these calixarene-tethered Ru^{II}(TAP) complexes, but the TA observed at 510 nm in a few tens of microseconds was too weak for analysis (Figure S62 in the Supporting Information).[48] With the deuterated complex **14**, the intramolecular quenching rate constant k_{qi} is equal to 0.51×10^6 s^{-1} instead of 0.77×10^6 s^{-1} (Table 2B); thus, with $k_{qi}(H)/k_{qi}(D) = 1.5$. We have to note that these values are rough approximations because, for calculation of k_{qi} ($k_{qi} = 1/\tau_{av} - 1/\tau_0$), we are forced to use an average lifetime (τ_{av}) and the τ_0 value of the free complex. Actually, the different lifetimes originate probably from the different distances or relative geometries between the phenol groups and the complex.

DISCUSSION AND CONCLUSION

We have developed different synthetic strategies to introduce one phen or one pytz unit on a calix[4 or 6]arene platform. These calixarene-based ligands were complexed with ruthenium(II) precursors to obtain new calixarene-based ruthenium(II) complexes. Examination of the electrochemical properties and the behavior under illumination of these new complexes constitute an important prerequisite for their use with biological systems.

The electrochemical and spectroscopic data clearly show that the calixarene-based Ru^{II}(TAP) complexes **7**, **14**, **19**, and **24** have kept their excellent oxidizing power under illumination (Table 1; E_{red}*), which has even slightly increased compared to the reference complex **25**. However, in the case of **7**, **14**, and **19**, data processing of the emission parameters indicates that an intramolecular luminescence quenching is present and can be attributed to the phenol groups of the calixarene subunit. Such intramolecular quenching is not present for **24** with azido groups.

The quenching has been characterized by Stern–Volmer and flash-photolysis experiments with the reference complex **25** in the presence of phenol. The fact that the 510 nm transient (i) is typical of the absorption of the reduced complex, (ii) occurs with a pseudo-first-order process in agreement with the value of the quenching rate constant, and (iii) decays according to a

dx.doi.org/10.1021/ic401468t | Inorg. Chem. 2013, 52, 11228–11236

bimolecular equimolecular process, because of back electron transfer between the reduced complex and oxidized phenol,[49] constitutes an excellent signature of the photoinduced ET process. We can thus assume that such an ET is also valid for the calixarene-based Ru^{II}(TAP) complexes.

The standard Gibbs energy (ΔG°) for this process has been estimated for **7**, **14**, and **19** to +0.32−0.34 eV from eq 1.1. It is slightly endergonic, as predicted from the low k_q value. This ET process can be assisted by a proton transfer because both the excited and reduced complexes are more basic than the starting complex.[44] Such an ET assisted by HT is also in agreement with the lower quenching rate constant value in the case of deuterated phenol. This is true for the free complex like for the calixarene-based Ru^{II}(TAP) complexes. It has been reported in the literature that, in the case of $[Ru(bpz)_3]^{2+}$,[45] an ET between the excited state of the $[Ru(bpz)_3]^{2+}$ and phenol derivatives is favored by a PCET in which not only the redox potentials but also the basicity of the excited complex and acidity of the electron donor have to be considered. The calculation of ΔG_{PCET}° for the PCET in the present case includes too many errors and uncertainties (E_{red}*, pK_a in MeCN, oxidation of phenol moieties of calixarene) for reporting reliable values (Figure S63 in the Supporting Information). We can, however, conclude that the phenolic protons probably participate in the ET process, but from the ratios $k_{qi}(H)/k_{qi}(D)$, which are rather weak, it is difficult to conclude whether the processes are concerted or not.

$$\Delta G_{ET}^\circ = -nF[E_{red}^*(Ru^{II}/Ru^{I}) - E_{ox}(PhOH/PhOH^{\bullet+})] \quad (1.1)$$

Equation 1.1 indicates the calculation of ΔG° for ET from phenol to the excited complex. For this estimation, we used the values of E_{red}* in Table 1 and an oxidation potential for the phenol moiety of +1.55 V vs SCE.[50]

It should be noted that a PCET has already been mentioned in the literature for Ru^{II}(TAP) complexes, but in that case, the donor was a guanine base of DNA.[51]

After the PCET, the back-reaction between the reduced (protonated or nonprotonated species) and oxidized species can take place as indicated by the bimolecular equimolecular decay of TA for the free complex and phenol (Figure 4). In this case, in competition with this reaction, the phenoxy radicals can probably dimerize or polymerize, as is described in the literature for other systems.[52] This is indeed compatible with the remaining absorption after the TA decay (Figure 4). If we extend this behavior to the calixarene-based Ru^{II}(TAP) complexes, we have to conclude that **7**, **14**, and **19**, thus with intramolecular luminescence quenching, are not good candidates to be used as photoreagents. Indeed, not only the direct PCET but also possible secondary photoreactions should decrease the efficiency of photodamaging by the Ru^{II}(TAP) calixarenes. This would not be the case for **24**, in which intramolecular quenching is absent. Complex **24** constitutes thus an attractive photoreagent for biomolecules because its high photooxidizing power would allow an ET to occur with biomolecular systems.[53] However, because it is poorly soluble in water, **24** could be used for in vitro analyses of cellular systems, but in that case with a mixture of water/organic solvent. Moreover, complex **24** could also be derivatized with groups favoring its solubility.[54] This opens new horizons for future applications; moreover, this complex constitutes a very promising precursor in order to develop multivalent and photoreactive metal compounds for targeting specific cell receptors thanks to multivalent recognition models.

■ ASSOCIATED CONTENT

Supporting Information

Additional spectra, cyclic voltammetry, Stern−Volmer experiments, deuteration of the phenol moiety, and equation for ΔG_{PCET}°. This material is available free of charge via the Internet at http://pubs.acs.org.

■ AUTHOR INFORMATION

Corresponding Authors

*E-mail: ijabin@ulb.ac.be. Fax: +32-2650-2798.
*E-mail: cmouche@ulb.ac.be. Fax: +32-2650-3018.
*E-mail: akirsch@ulb.ac.be. Fax: +32-2650-3018.

Notes

The authors declare no competing financial interest.

■ ACKNOWLEDGMENTS

The authors thank the FRFC-FNRS for financial support. A.M. and L.M. are grateful to the FNRS for Ph.D. grants. A.M. is also grateful to the David & Alice Van Buuren Funds for a complementary Ph.D. grant.

■ REFERENCES

(1) Nazeeruddin, M. K.; Grätzel, M. In *Transition Metal Complexes for Photovoltaic and Light Emitting Applications. In Photofunctional Transition Metal Complexes*; Yam, V. W. W., Ed.; Springer: Heidelberg, Germany, 2007; Vol. *123*, pp 113−175.
(2) Puntoriero, F.; Nastasi, F.; Cavazzini, M.; Quici, S.; Campagna, S. *Coord. Chem. Rev.* **2007**, *251*, 536−545.
(3) Rau, S.; Walther, D.; Vos, J. G. *Dalton Trans.* **2007**, 915−919.
(4) Balzani, V.; Campagna, S.; Denti, G.; Juris, A.; Serroni, S.; Venturi, M. *Sol. Energy Mater. Sol. Cells* **1995**, *38*, 159−173.
(5) Ortmans, I.; Moucheron, C.; Kirsch-De Mesmaeker, A. *Coord. Chem. Rev.* **1998**, *168*, 233−271.
(6) Lo, K. K.-W. Luminescent transition metal complexes as biological labels and probes. In *Photofunctional Transition Metals Complexes*; Yam, V. W. W., Ed.; Springer-Verlag: Berlin, 2007; Vol. *123*, pp 205−245.
(7) Pierard, F.; Kirsch-De Mesmaeker, A. *Inorg. Chem. Commun.* **2006**, *9*, 111−126.
(8) Metcalfe, C.; Thomas, J. A. *Chem. Soc. Rev.* **2003**, *32*, 215−224.
(9) Erkkila, K. E.; Odom, D. T.; Barton, J. K. *Chem. Rev.* **1999**, *99*, 2777−2796.
(10) Nordén, B.; Lincoln, P.; Akerman, B.; Tuite, E. *Met. Ions Biol. Syst.* **1996**, *33*, 177−252.
(11) Le Gac, S.; Rickling, S.; Gerbaux, P.; Defrancq, E.; Moucheron, C.; Kirsch-De Mesmaeker, A. *Angew. Chem., Int. Ed.* **2009**, *48*, 1122−1125.
(12) Marcélis, L.; Ghesquière, J.; Garnir, K.; Kirsch-De Mesmaeker, A.; Moucheron, C. *Coord. Chem. Rev.* **2012**, *256*, 1569−1582.
(13) Moucheron, C.; Kirsch-De Mesmaeker, A.; Kelly, J. M. *J. Photochem. Photobiol., B* **1997**, *40*, 91−106.
(14) Moucheron, C.; Kirsch-De Mesmaeker, A.; Kelly, J. M. Photophysics and photochemistry of metal polypyridyl and related complexes with nucleic acids. *Less Common Metals in Proteins and Nucleic Acid Probes*; Springer: Berlin, 1998; Vol. *92*, pp 163−216.
(15) Elias, B.; Kirsch-De Mesmaeker, A. *Coord. Chem. Rev.* **2006**, *250*, 1627−1641.
(16) Herman, L.; Ghosh, S.; Defrancq, E.; Kirsch-De Mesmaeker, A. *J. Phys. Org. Chem.* **2008**, *21*, 670−681.
(17) Jacquet, L.; Kelly, J. M.; Kirsch-De Mesmaeker, A. *J. Chem. Soc., Chem. Commun.* **1995**, 913−914.
(18) Jacquet, L.; Davies, R. J. H.; Kirsch-De Mesmaeker, A.; Kelly, J. M. *J. Am. Chem. Soc.* **1997**, *119*, 11763−11768.

(19) Puckett, C. A.; Barton, J. K. *J. Am. Chem. Soc.* **2007**, *129*, 46−47.
(20) Puckett, C. A.; Barton, J. K. *Bioorg. Med. Chem.* **2010**, *18*, 3564−3569.
(21) Mattiuzzi, A.; Jabin, I.; Moucheron, C.; Kirsch-De Mesmaeker, A. *Dalton Trans.* **2011**, *40*, 7395−7402.
(22) For a review about calixarenes, see: Rowan, , A. E.; Rowan, , S. J.; Aida, , T.; Gutsche, , C. D. *Calixarenes: An Introduction*, 2nd ed.; The Royal Society of Chemistry: London, **2008**,; pp P001−−P276.
(23) For a review about ruthenium(II) calixarene complexes, see: Beer, P. D.; Hayes, E. J. *Coord. Chem. Rev.* **2003**, *240*, 167−189.
(24) Nimse, S. B.; Kim, T. *Chem. Soc. Rev.* **2013**, *42*, 366−386.
(25) Bagnacani, V.; Sansone, F.; Donofrio, G.; Baldini, L.; Casnati, A.; Ungaro, R. *Org. Lett.* **2008**, *10*, 3953−3956.
(26) Sansone, F.; Baldini, L.; Casnati, A.; Ungaro, R. *New J. Chem.* **2010**, *34*, 2715−2728.
(27) Baldini, L.; Casnati, A.; Sansone, F.; Ungaro, R. *Chem. Soc. Rev.* **2007**, *36*, 254−266.
(28) Mammen, M.; Choi, S.-K.; Whitesides, G. M. *Angew. Chem., Int. Ed.* **1998**, *37*, 2754−2794.
(29) Sullivan, B. P.; Salmon, D. J.; Meyer, T. J. *Inorg. Chem.* **1978**, *17*, 3334−3341.
(30) Evans, I. P.; Spencer, A.; Wilkinson, G. *J. Chem. Soc., Dalton Trans.* **1973**, 204−209.
(31) Biffin, M. E. C.; Miller, J.; Paul, D. B. Introduction of the Azido Group. *The Azido Group (1971)*; John Wiley & Sons, Ltd.: New York, 2010; pp 57−190.
(32) Casnati, A.; Arduini, A.; Ghidini, E.; Pochini, A.; Ungaro, R. *Tetrahedron* **1991**, *47*, 2221−2228.
(33) Groenen, L. C.; Ruël, B. H. M.; Casnati, A.; Verboom, W.; Pochini, A.; Ungaro, R.; Reinhoudt, D. N. *Tetrahedron* **1991**, *47*, 8379−8384.
(34) Sénèque, O.; Reinaud, O. *Tetrahedron* **2003**, *59*, 5563−5568.
(35) Darbost, U.; Zeng, X.; Giorgi, M.; Jabin, I. *J. Org. Chem.* **2005**, *70*, 10552−10560.
(36) Zeng, C.-C.; Becker, J. Y. *Tetrahedron* **2004**, *60*, 1643−1650.
(37) Deroo, S.; Defrancq, E.; Moucheron, C.; Kirsch-De Mesmaeker, A.; Dumy, P. *Tetrahedron Lett.* **2003**, *44*, 8379−8382.
(38) Demko, Z. P.; Sharpless, K. B. *Org. Lett.* **2001**, *3*, 4091−4094.
(39) Ortmans, I.; Elias, B.; Kelly, J. M.; Moucheron, C.; Kirsch-De Mesmaeker, A. *Dalton Trans.* **2004**, 668−676.
(40) Leveque, J.; Elias, B.; Moucheron, C.; Kirsch-De Mesmaeker, A. *Inorg. Chem.* **2005**, *44*, 393−400.
(41) Boisdenghien, A.; Moucheron, C.; Kirsch-De Mesmaeker, A. *Inorg. Chem.* **2005**, *44*, 7678−7685.
(42) Hager, G. D.; Crosby, G. A. *J. Am. Chem. Soc.* **1975**, *97*, 7031−7037.
(43) Kirsch-De Mesmaeker, A.; Jacquet, L.; Nasielski, J. *Inorg. Chem.* **1988**, *27*, 4451−4458.
(44) Herman, L.; Elias, B.; Pierard, F.; Moucheron, C.; Kirsch-De Mesmaeker, A. *J. Phys. Chem. A* **2007**, *111*, 9756−9763.
(45) Bronner, C.; Wenger, O. S. *J. Phys. Chem. Lett.* **2012**, *3*, 70−74.
(46) Kirsch-De Mesmaeker, A.; Lecomte, J.-P.; Kelly, J. M. Photoreactions of metal complexes with DNA, especially those involving a primary photoelectron transfer. In *Electron Transfer II*; Mattay, J., Ed.; Springer: Berlin, 1996; Vol. *177*, pp 25−76.
(47) It was checked that excited **25** is not quenched by anisole up to concentrations of 500 mM in MeCN. Moreover, the k_{qi} value for **14** (with two phenol groups) is smaller than that for **7** (with three phenol groups). These data indicate thus that intramolecular quenching is controlled by the phenol units.
(48) The concentration was not increased to avoid possible intermolecular quenching, which would prevent simple kinetic analysis of the calixarene system.
(49) Lecomte, J.-P.; Kirsch-De Mesmaeker, A.; Feeney, M. M.; Kelly, J. M. *Inorg. Chem.* **1995**, *34*, 6481−6491.
(50) Izutsu, K. *Electrochemistry in Nonaqueous Solutions*; Wiley-VCH Verlag GmbH & Co. KGaA: New York, 2003.
(51) Elias, B.; Kelly, J. M.; Creely, C.; Doorley, G. W.; Feeney, M. M.; Moucheron, C.; Kirsch-De Mesmaeker, A.; Dyer, J.; Grills, D. C.; George, M. W.; Matousek, P.; Parker, A. W.; Towrie, M. *Chem.—Eur. J.* **2008**, *14*, 369−375.
(52) Kobayashi, S.; Higashimura, H. *Prog. Polym. Sci.* **2003**, *28*, 1015−1048.
(53) The equivalent of **24** with calix[4]arene exhibited decomposition during synthesis; therefore, it could not be studied.
(54) For a review about water-soluble calixarenes, see: Casnati, A.; Sciotto, D.; Arena, G. Water-soluble calixarenes. In *Calixarenes*; Asfari, Z., et al., Eds.; Kluwer Academic Publishers: Dordrecht, The Netherlands, 2001; pp 440−456.